Isı Bilimi ve Tekniği Dergisi, 35, 1, 1-9, 2015
J. of Thermal Science and Technology

ISSN 1300-3615

HYDRODYNAMIC CHARACTERISTICS OF TWO-PHASE FLOW THROUGH HORIZONTAL PIPE HAVING SMOOTH EXPANSION

Emrah DENİZ* and Nurdil ESKİN**
*Istanbul Technical University, Faculty of Mechanical Engineering
34437 Beyoglu, Istanbul, Turkey, emrah.deniz@itu.edu.tr
**Istanbul Technical University, Faculty of Mechanical Engineering
34437 Beyoglu, Istanbul, Turkey, eskinn@itu.edu.tr

(Geliş Tarihi: 23.09.2013, Kabul Tarihi: 18.02.2014)

Abstract: In this study, characteristics of adiabatic two-phase flow through horizontal pipe having smooth expansion are investigated numerically and experimentally. Effects of volumetric void fraction and internal diameter of the pipe on hydrodynamic characteristics of the two-phase flow are examined using average diameter of the bubbles injected. Air and water are chosen as the fluid couple. Flow rate for water is kept constant at 3 lt/s while those for air are taken as 50 and 61 lt/min. Thus, volumetric void fraction of 21.74 and 25.31 % are obtained for the two-phase flow considered, respectively. Eulerian-Eulerian Model and Reynolds Stress Model (RSM) are employed for modeling of two-phase flow and turbulence. Numerical results are then compared to the experimental data that was previously obtained by dual optical probe that measures local parameters of the two-phase flow (Deniz, 2009). The comparison shows that using the assumption of the average bubble diameter for numerical modeling gives reasonable results for developed and stratified flow.
Keywords: Two-phase flow, Numerical simulation, Dual optical probe, Smooth expansion, Void fraction, Pressure drop

TEDRİCİ GENİŞLEMEYE SAHİP YATAY BORU BOYUNCA İKİ FAZLI AKIŞIN HİDRODİNAMİK KARAKTERİSTİĞİ

Özet: Bu çalışmada, tedrici genişlemeye sahip yatay kanaldan geçen adyabatik iki fazlı akışın karakteristikleri sayısal ve deneysel olarak incelenmiştir. Hacimsel boşluk oranı ve boru iç çapının iki fazlı akış karakteristiğine etkisi, enjekte edilen kabarcıkların ortalama çapı kullanılarak irdelenmiştir. Akış çifti olarak hava ve su seçilmiştir. Hacimsel debi değerleri, su için 3 lt/s; hava için 50 ve 61 lt/dak olarak alınmıştır. Böylece incelenen iki fazlı akıştaki hacimsel boşluk oranı değerleri sırasıyla % 21.74 ve % 25.31 olarak elde edilmiştir. İki fazlı akışın ve türbülansın modellenmesinde Euler-Euler Modeli ve Reynolds Gerilim Modeli kullanılmıştır. Sayısal sonuçlar, iki fazlı akışın yerel parametrelerini ölçen ikili optik prop kullanarak, daha önceden elde edilen deneysel sonuçlarla karşılaştırılmıştır (Deniz, 2009). Karılaştırma sonucunda, sayısal modellemede kullanılan ortalama kabarcık çapı yaklaşımının gelişmiş ve katmanlaşmış akış için kabul edilebilir sonuçlar verdiği bulunmuştur.
Anahtar Kelimeler: İki fazlı akış, Sayısal modelleme, İkili optik prop, Tedrici genişleme, Boşluk oranı, Basınç düşüşü

NOMENCLATURE

A	Area [m^2]
D	Diameter [m]
f	Friction factor
s	Mass flux [kg/m^2s]
g	Gravitational acceleration [m/s^2, cm/s^2]
k	Turbulence kinetic energy [m^2/s^2]
L	Length [m]
N	Number of the holes in the injector
P	Pressure [Pa]
S	Slip ratio [U_G/U_L]
u,U	Velocity [m/s]
V	Volume [cm^3]
x	Quality[m_{pas}/m_{total}]
y	Position on the y-axis [m]
$\dot{Q}$	Volumetric flow rate [m^3/s]

Greek Symbols

α	Void fraction [A_g/A_{total}]
β	Volumetric void fraction [$\dot{Q}_{gas}$ / $\dot{Q}_{total}$]
ε	Turbulence dissipation [m^2/s^3]
ε	Surface roughness [m]
μ	Dynamic viscosity [$Pa.s$]
υ,ν	Kinematic viscosity [cm^3/s, m^2/s]
ρ	Density [kg/m^3]
Φ	Two phase flow factor
X	Lockhart-Martinelli factor

Subscripts

l	Liquid phase
g	Gas phase

INTRODUCTION

Gas-liquid two-phase flow takes the leading role in applications including evaporation, condensation and flow through cross-sectional area change (i.e. nozzle, diffuser) and sudden pressure drop (i.e. flashing). These systems normally have complex geometries composed by singularities like expansion, contraction, bends, orifices, etc. Thus, two-phase flow characteristics, such as distribution of local void fraction and phase velocities, pressure drop and flow pattern of aforementioned singularities should be identified for design of such systems. However, there is limited research documented in this subject. Theoretical analyses of air-water flow through straight horizontal and/or vertical pipe and comparison of results with experiments were performed by Ekambara et al. (2008), Ghorai et al. (2006), Morel et al. (2010) and Chahed et al. (2003). The effects of phase velocities, volume fraction of gas and interfacial roughness on two-phase flow characteristics were investigated in these studies. Winterton et al. (2001), Ahmed et al. (2008), Aloui et al. (1999) and Balakhrisna et al. (2010), researched two-phase flow through straight pipes with or without sudden expansion, while Fossa and Guglielmini (1998) and Bertola (2004) worked on pies with sudden contraction, experimentally. They used instruments such as electrical impedance probe (Fossa and Guglielmini 1998), hot-film anemometer (Ahmed et al. 2008), fiber optical probe (Bertola 2004), and CCD camera (Winterton et al. 2001) for measurements. Winterton et al. (2001), Aloui et al. (1999) and Fossa and Guglielmini (1998) performed local measurements whereas Balakhrisna et al. (2010) measured average. Liquid couples that were studied were air-oil (Ahmed et al. 2008), water-air (Ekambara et al. 2008, Ghorai et al. 2006, Morel et al. 2010, Chahed et al. 2003, Winterton et al. 2001, Aloui et al. 1999, Fossa and Guglielmini 1998, Bertola 2004) and oil-water (Balakhrisna et al. 2010).

As summarized above, it can be seen in literature that the numerical and/or experimental studies investigating the gas-liquid flow characteristics generally contain flow through straight pipes or pipes with abrupt changes. There are only few studies considering the progressive cross-sectional changes. Additionally, except the ones listed above, it can be stated that the majority of the experimental studies published in the literature consists of averaged values of two-phase flow parameters. One also can note that many theoretical studies are validated by referring to the averaged experimental values although they are constructed on the separated flow model that provides the local values. Therefore, the theoretical investigation of two-phase flow through singular geometries and its validation with local measurements is a gap in literature that needs to be addressed.

In this study, characteristics of adiabatic air-water two-phase flow through horizontal pipe with progressive expansion are investigated. Results of the theoretical analysis based on Eulerian-Eulerian model are compared with the data that was previously obtained by using dual optical probe (Deniz, 2009). Construction of the numerical domain and the analysis are performed in GAMBIT (v. 2.3.16) and ANSYS FLUENT (v. 12), respectively. For simulations, the average diameter of the bubbles injected to the flow is calculated via a correlation proposed by Kunii (1991). Referring to the comparison with the experimental results, it can be concluded that the presented model based on average bubble diameter can describe the local values and the flow pattern reasonably.

EXPERIMENTAL SETUP

The schematic representation of the experimental facility is given in Figure 1. Water and air were chosen as the fluid couple. Water at atmospheric conditions was taken from the tank by a pump and sent to the pipe attached to an electro-magnetic type flow meter in order to measure its volumetric flow rate, $\dot{Q}(m^3/s)$. Meanwhile air at the atmospheric conditions was compressed by the compressor and delivered to an immersed injector where the two-phase flow was obtained. It had 28 holes with 1 mm diameter positioned on four rods inserted through the cross-section of the upstream pipe inlet. Air-water mixture then flowed through the test section where the measurements were performed by optical probe. Accuracy of the probe is given as ± 7 % by the manufacturer company, RBI (France). Measurement principles of the optical probe can be found in François et al (2003). All pipes in the facility are made of transparent acrylic in order to observe the flow. Picture of the injector and schematic of the test section are shown in Figure 2.

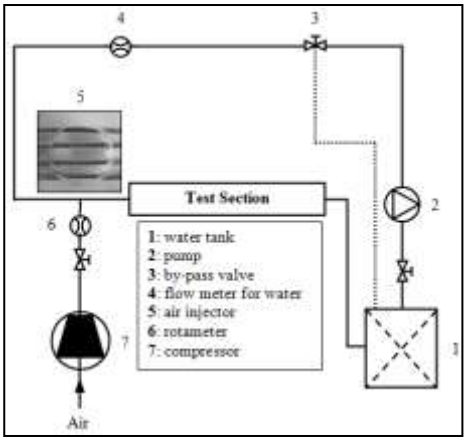

Figure 1. Schematic of the experimental facility

The test section consisted of three pipes called upstream pipe, singularity pipe and downstream pipe with prescribed length and diameters. Inner diameter of the upstream channel (i.e. 32 mm) enlarged to that of the downstream channel (i.e. 40 mm) smoothly, with an expansion angle of 9°. Area ratio for the singularity was calculated to be 0.64. In the measurements, flow rate of water was taken as 3 l/s, while that of air were 50 and 61 l/min. Thus, volumetric void fractions of 21.74 and 25.31 % were achieved for the flow, respectively.

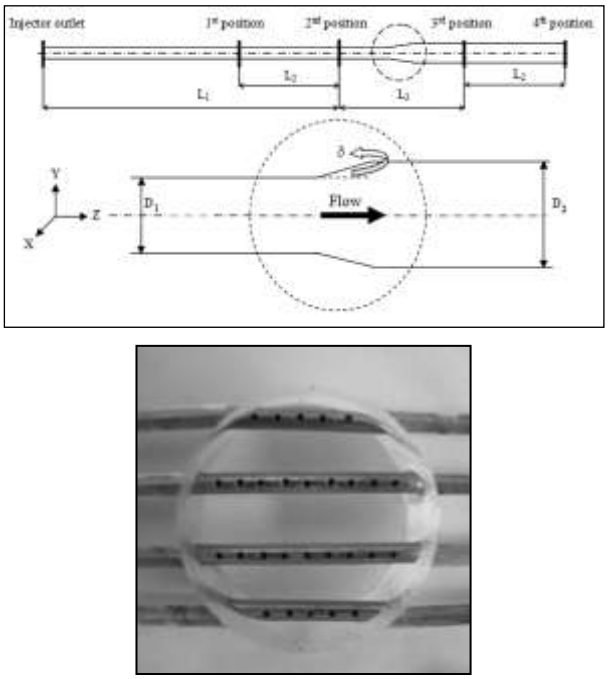

Figure 2. Test section and the injector used in the experimental study

As shown in Figure 2, there are four locations where experimental and numerical results are compared, two at the inlet and outlet of the singularity pipe, and the other two at $10 \times D_1$ (i.e. 320 mm) before and after the former ones. For clarity, these locations of these positions will be defined in terms of γ, throughout the text, γ being the distance from the injector divided by the total length of the test section. Thus, from first location to the forth, γ takes the values of 0.4, 0.58, 0.82 and 1, respectively. The geometrical details of the test section and the operational conditions are given in Table 1**.**

Table 1. Operating conditions of the experimental study

Geormetry	L_1 = 1000 mm L_2 = 320 mm L_3 = 410 mm D_1 = 32 mm D_2 = 40 mm
Gas phase/Liquid phase	Air/water at atmospheric conditions
$\dot{Q}_{air}$ / $\dot{Q}_{water}$	50 and 61 [l/min] / 3 [l/s]
β	21.74 % and 25.31 %

THEORETICAL MODEL

Governing Equations

In this study, the simulation of air-water flow through the test section is performed by two-fluid Eulerian-Eulerian model at steady-state condition. Considering no mass transfer between the phases and no heat transfer from the surroundings to the flow or vice versa, the governing equations of the model are given below.

$$u_l = \bar{u}_l + u_l' \tag{1}$$

$$u_g = \bar{u}_g + u_g' \tag{2}$$

$$\rho_l \nabla\left[(1-\alpha) u_l A\right] = 0 \tag{3}$$

$$\rho_g \nabla\left[\alpha u_g A\right] = 0 \tag{4}$$

$$\rho_l u_l \nabla(u_l(1-\alpha)) = -\nabla P(1-\alpha) - \rho_l g \sin\theta(1-\alpha) + F_1 \tag{5}$$

$$\rho_g u_g \nabla(u_g \alpha) = -\nabla P(\alpha) - \rho_g g \sin\theta(\alpha) - F_2 \tag{6}$$

For modeling of turbulence, Reynolds Stress Model (RSM) is utilized in the simulations. The exact equations used in the model are given below.

$$\frac{D\overline{u_i' u_j'}}{Dt} = \frac{\partial}{\partial X_k}\left(-\overline{u_i' u_j' u_k'} - \overline{\frac{p}{\rho}\left(\delta_{jk} u_i' + \delta_{ik} u_j'\right)} + \upsilon \frac{\partial \overline{u_i' u_j'}}{\partial X_k}\right) - \left(\overline{u_i' u_j'} \frac{\partial \bar{u}_j}{\partial X_k} + \overline{u_j' u_k'} \frac{\partial \bar{u}_i}{\partial X_k}\right) - 2\upsilon \overline{\frac{\partial u_i'}{\partial X_k} \frac{\partial u_j'}{\partial X_k}} + \overline{\frac{p}{\rho}\left(\frac{\partial u_i'}{\partial X_j} + \frac{\partial u_j'}{\partial X_i}\right)} \tag{7}$$

$$\frac{Dk}{Dt} = \frac{\partial}{\partial X_k}\left(-\overline{u_k'\left(k' + \frac{p}{\rho}\right)} + \upsilon \frac{dk}{dX_k}\right) - \overline{u_i' u_k'} \frac{\partial \bar{u}_i}{\partial X_k} - \varepsilon \tag{8}$$

$$\frac{D\varepsilon}{Dt} = \frac{\partial}{\partial X_k}\left(-\overline{\varepsilon' u_k'} - \frac{2\upsilon}{\rho} \overline{\frac{\partial u_k'}{\partial X_j} \frac{\partial p}{\partial X_j}} + \upsilon \frac{\partial \varepsilon}{\partial X_k}\right) - 2\upsilon \frac{\partial \bar{u}_i}{\partial X_j}\left(\frac{\partial u_k'}{\partial X_i} \frac{\partial u_k'}{\partial X_j} + \frac{\partial u_i'}{\partial X_k} \frac{\partial u_j'}{\partial X_k}\right) - 2\upsilon \overline{u_l' \frac{\partial u_i'}{\partial X_j}} \frac{\partial^2 \bar{u}_i}{\partial X_k \partial X_j} - 2\upsilon \overline{\frac{\partial u_i'}{\partial X_j} \frac{\partial u_i'}{\partial X_k} \frac{\partial u_j'}{\partial X_k}} - 2\overline{\left(\upsilon \frac{\partial^2 u_i'}{\partial X_k \partial X_j}\right)^2} \tag{9}$$

Numerical Analysis

The numerical analysis of the flow under consideration is performed based on the parameters and the geometrical restrictions mentioned in the experimental setup section of this paper. Since characteristics of the bubbles in two-phase flow are determined by the design parameters of the injector utilized in the experimental study (Figure 2.), the numerical analysis in the present study is performed in two steps including the simulation of the flow through the injector, and then through the pipes.

Modeling of the flow through the injector

The numerical geometry constructed for the injector is given in Figure 3. Here, the holes of the injector are represented by the means of rods of 32 mm length that are inserted to a pipe, which was all created within 3D domain. In order to ease the step of creating the structural

mesh, the rods are constructed with square cross-sections having the same hydraulic diameter with that of the circular holes, i.e. 1 mm. According to the simulation, air flows through these rods while water enters the pipe from the remaining cross-section at the inlet, and the two-phase flow of interest is obtained just after the outlet of the rods where the phases infiltrate each other. At the end of the simulation for each air flow rate, the phase velocity, and the void fraction profiles obtained at the downstream of the rods are extracted from the simulation, and are introduced as the inlet conditions for the analysis of the flow through the pipes.

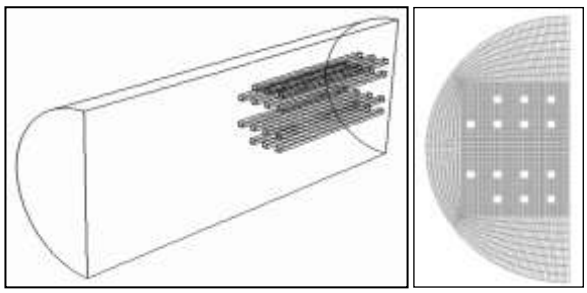

Figure 3. Numerical geometry of the injector (left) and mesh structure at water-inlet

370,000 nodes are considered adequate for the injector simulation according to the grid independency examination performed by testing several domains with different node densities. The mesh structure at water-inlet is also shown in Figure 3. In ANSYS FLUENT (v.12), the boundary condition "velocity inlet" is taken as the inlet condition for water and air, while the boundary conditions "interior" and "outflow" are employed as the outlet condition for the rods and the pipe, respectively. It was only needed to model the half of the injector by using the symmetry condition. Eulerian multiphase model is used for the analysis. Reynolds Stress Model (RSM) is employed to model the turbulent flow. Standard Wall Functions are utilized for near wall treatment. Phase Coupled SIMPLE scheme for pressure-velocity coupling, Green-Gauss Cell Based option for gradients, and Second Order Upwind for spatial discretization are chosen.

Modeling of the flow through the pipes

The second step of the analysis is modeling of the two-phase flow through the test section having three regions, i.e. upstream, through and downstream of the singularity. The numerical domain of the system is constructed in 3D, and is symmetrical with respect to y-axis. 83,817 nodes are determined to be adequate for upstream and downstream pipes, while twice the nodes are used for the singularity section, according to the grid independency study. In each region, the axial length in z-direction is divided into 400 pieces. For the upstream pipe, the node densities in y-direction for each grid of the independency study, and the corresponding void fraction distributions are given in Figure 4 and Figure 5.

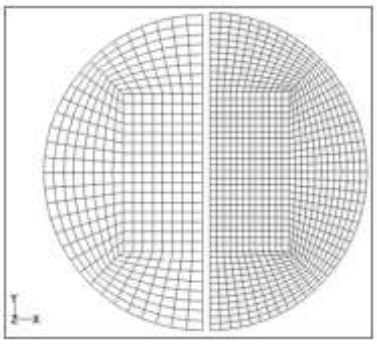

Figure 4. y-directional node densities for the tested grids having 83,817 (left) and 185,513 (right) nodes

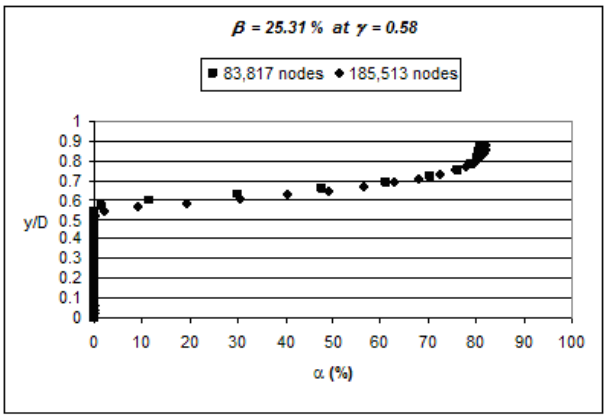

Figure 5. Grid independency test based on void fraction distribution

In order to determine the turbulence model to be used, flow through the upstream pipe is modeled via Standard k-ε and Reynolds Stress Model (RSM), and is compared with the related experimental results illustrated in Figure 6. According to the comparison, RSM turbulence model is chosen for the numerical simulation of the flow considered. As in the injector simulation, Eulerian multiphase model is used for the analysis. Standard Wall Functions are utilized for near wall treatment. Phase Coupled SIMPLE scheme for pressure-velocity coupling, Green-Gauss Cell Based option for gradients, and Second Order Upwind for spatial discretization are chosen.

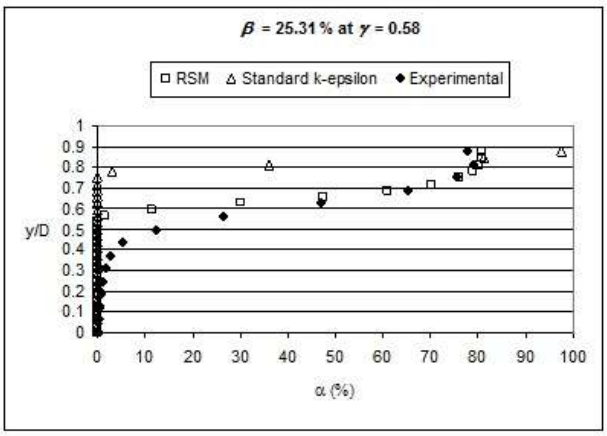

Figure 6. Comparison of turbulence models with the experimental data

Modeling of the bubbles

Due to momentum of the flow and forces between the phases, the injected bubbles break up or coalesce, causing a variation in bubble diameter along the flow. In this study, it is assumed that bubbles are spherical and that they do not interact with each other. By using the former assumption, an average diameter value for the bubbles at the injector outlet is extracted from the volume estimated via the correlation written in literature (Kunii 1991) and is given below.

$$V_{bubble} = 1.138 \frac{(\upsilon / N)^{6/5}}{g^{3/5}} \quad (10)$$

RESULTS AND DISCUSSIONS

Experimental Results

The experimental results for the radial distribution of the local void fraction along the upstream and downstream of the smooth expansion are plotted below. In the following figures, y/D stands for the non-dimensional position and is defined as the position on the y-axis divided by the channel diameter. Thus, y/D varies from zero to the unity representing the bottom and top of the channel, respectively.

The experimental values obtained at upstream of the smooth expansion are given in Figure 7 and Figure 8. From the figures, it can be seen that the local void fraction increases with increasing y/D value due to the density difference between air and water, and the effect of gravitational force. As the flow moves along the upstream pipe (towards γ = 0.58), the effect of volumetric void fraction becomes obvious at the top of the channel due to the development of stratification. As expected, local void fraction rises with increasing volumetric void fraction.

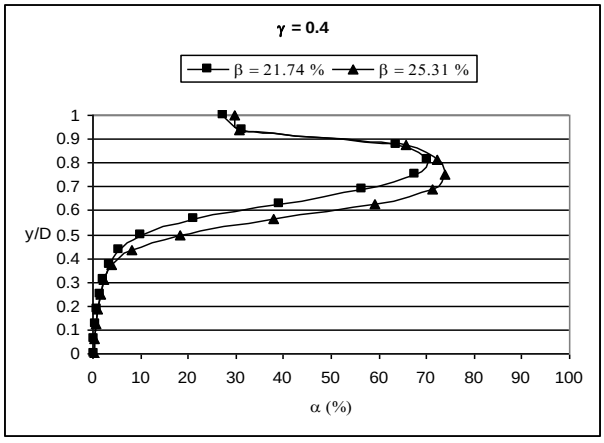

Figure 7. Effect of volumetric void fraction at $\gamma = 0.4$

The radial distribution of local void fraction at downstream of the smooth expansion is illustrated in Figure 9 and Figure 10. Once compared with the values obtained upstream of the expansion, it can be stated that the local void fraction values increase after the singularity location (i.e. γ = 0.82) since the velocity of the phases decreases with an increase in the cross-section of the pipe.

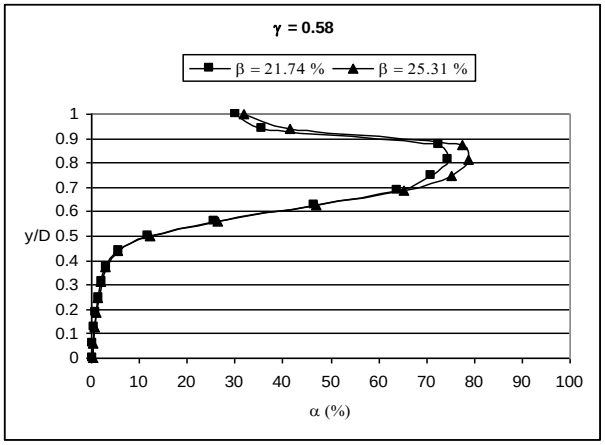

Figure 8. Effect of volumetric void fraction at $\gamma = 0.58$

The flow with lower volumetric void fraction decelerates more than that with the higher one. This effect becomes significant at top of the channel, where most of the bubbles gather. Thus, local void fraction values for $\beta = 21.74$ % are greater than those for $\beta = 25.31$ % a can be observed in Figure 9. The discrepancy decreases as the flow develops through the downstream pipe as shown in Figure 10.

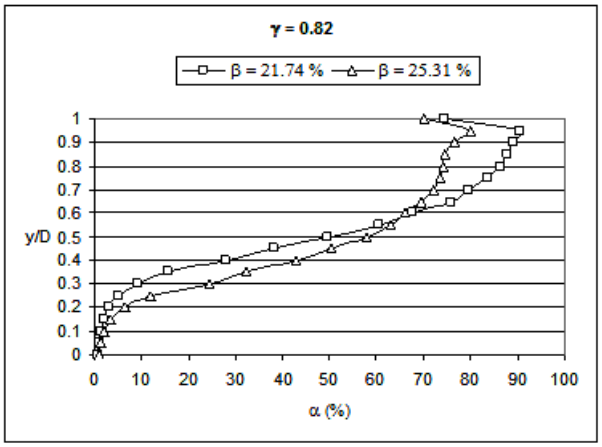

Figure 9. Effect of volumetric void fraction at $\gamma = 0.82$

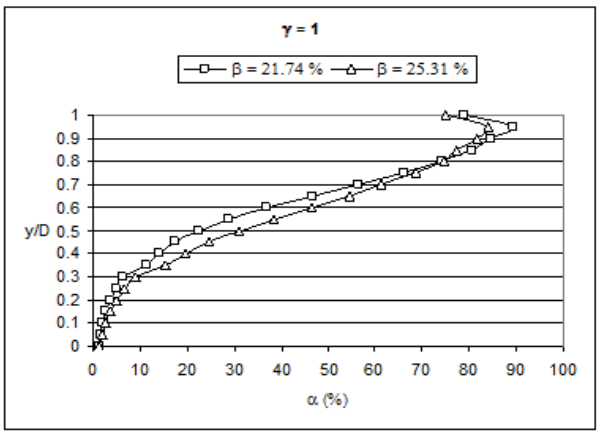

Figure 10. Effect of volumetric void fraction at $\gamma = 1$

Numerical Results

The numerical values of two-phase flow parameters along the radial direction of the pipes and their comparison with the experimental results are given in the following sections.

Radial Distribution of Void Fraction

The numerical and experimental local void fraction distributions for $\beta = 25.31$ % at $\gamma = 0.4$ and $\gamma = 0.58$ are shown in Figure 11 and Figure 12, respectively.

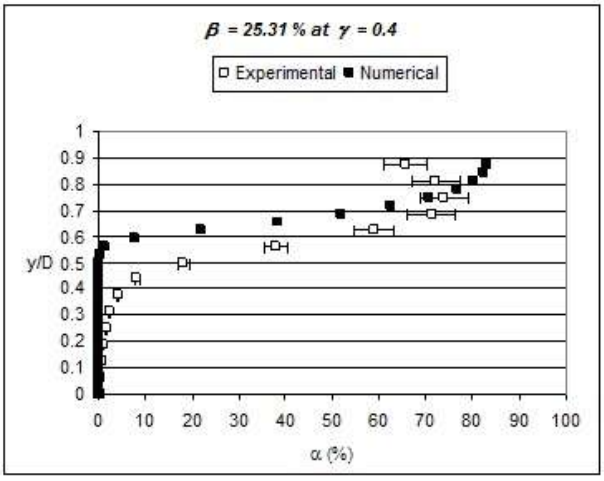

Figure 11. Local void fraction distribution at $\gamma = 0.4$

From the figures, it can be seen that the numerical and experimental values are comparable and are getting closer to each other as the flow develops. In a developing bubbly flow, the diameter of the bubbles are affected by the interactions (i.e. break-up, coalescence) and the forces (lift and drag) more than it does in a developed flow, and therefore more variation would be observed. Also, using the optical probe for experiments is an intrusive method that causes an error of ± 7 % in the measurements due to its blockage effect, contributing to the difference the numerical values. Referring to the explanations written above and to the comparison between the values plotted in Figure 11 and Figure 12, it can be concluded that the model based on the constant bubble diameter assumption simulates the developed and the stratified two-phase flow more successfully than that for the developing flow, for the cases investigated.

The numerical local void fraction distribution through the singularity pipe is plotted for $\beta = 21.74$ % in Figure 13. Stratified water-air flow enters the singularity pipe at $\gamma = 0.58$ and begins to decelerate at singularity-inlet ($\gamma = 0.69$) due to the smoothly enlarging cross-section. Since deceleration of water is greater than that of air due to the higher density of water, local void fraction values decrease, the stratification developed along the upstream pipe collapses, and the local void fraction distribution takes the form of a curve. The curve gets narrower as the decelerating continues along the singularity outlet ($\gamma = 0.7$). Then a new stratification begins to develop in the downstream pipe.

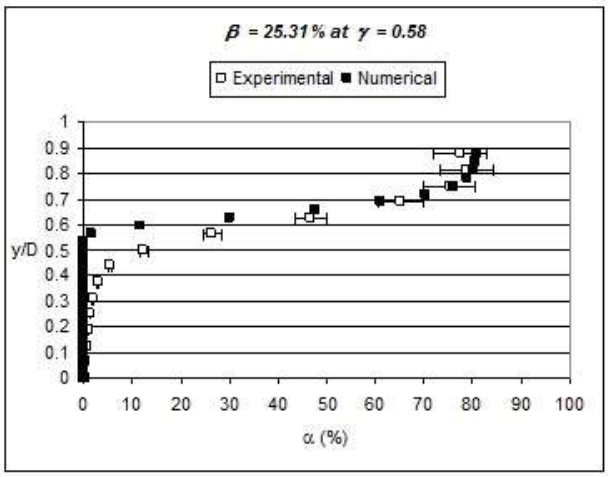

Figure 12. Local void fraction distribution at $\gamma = 0.58$

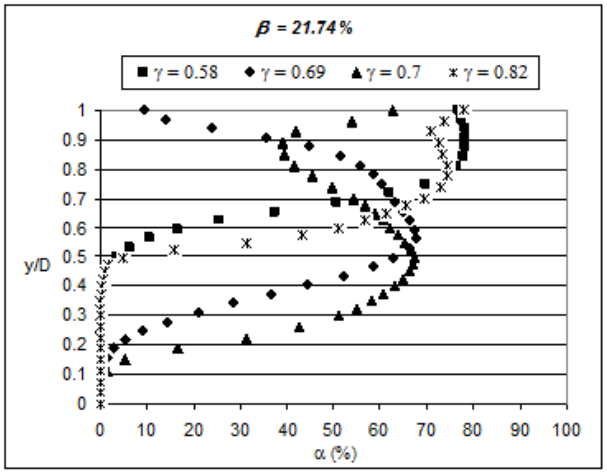

Figure 13. Numerical local void fraction distribution along the singularity pipe for $\beta = 21.74$ %

The numerical results for the downstream pipe are compared with the experimental results and the comparison is shown in Figure 14 and Figure 15.

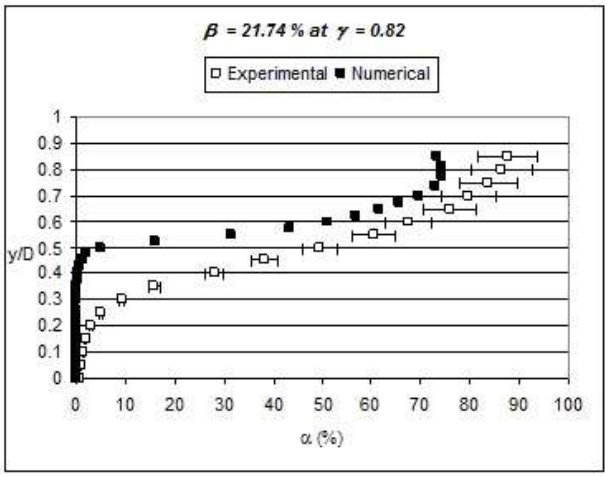

Figure 14. Local void fraction distribution at $\gamma = 0.82$

From Figure 14, it can be observed that the numerical simulation and the experimental measurements give similar profiles for the local void fraction distribution at downstream of the singularity. As the stratification develops, numerical and experimental values get closer to each other as seen in Figure 15. Furthermore, the stratification in the lower half of the downstream channel develops earlier in the numerical simulation as in the upstream pipe because of the constant bubble diameter assumption.

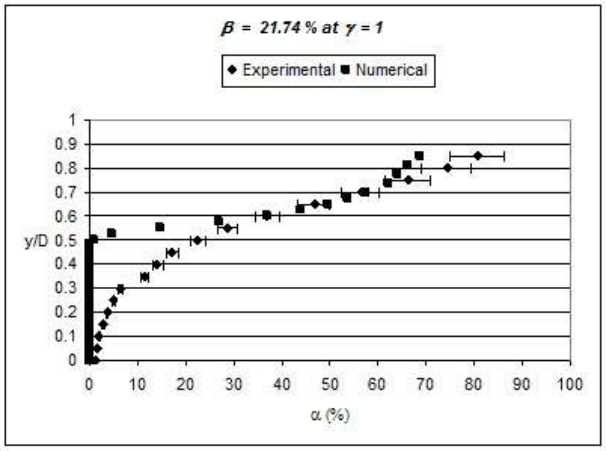

Figure 15. Local void fraction distribution at $\gamma = 1$

Slip Ratio

Slip ratio is an important parameter in two-phase flow since it determines the type of the model (i.e. homogeneous or separated) that the flow characteristics can be analyzed with. Slip ratio variation with respect to γ for $\beta = 21.74$ % and $\beta = 25.31$ % is given in Figure 16.

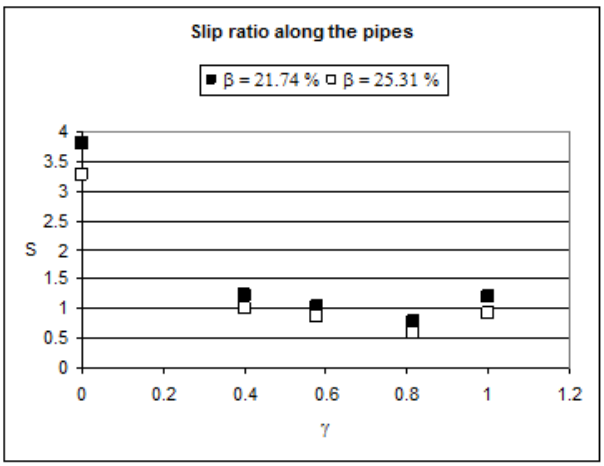

Figure 16. Variation of numerical slip ratio with respect to γ

For both cases shown in the figure, the slip ratio takes the maximum value at the injector outlet due to the high velocity of the air during injection. As the flow develops, S varies between 1.24 and 0.58. Thus, it can be concluded that the separated flow model must be used in order to analyze the flow characteristics, as is already performed in the present study. The effects of the singularity section and the volumetric void fraction on the local slip ratio distribution are given in Figure 17.

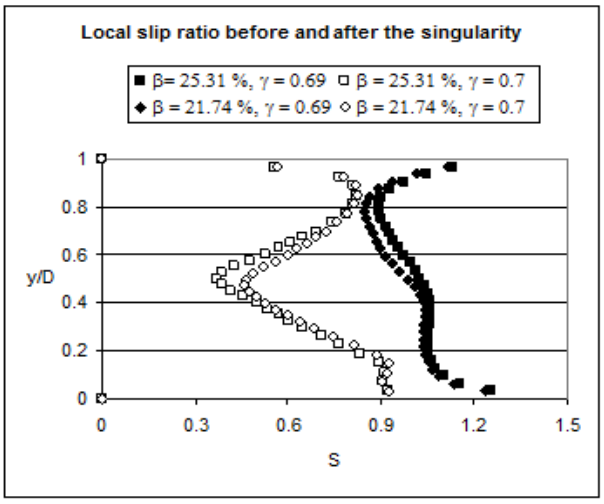

Figure 17. Distribution of numerical local slip ratio before and after the singularity

Two-Phase Pressure Drop

The numerical values for the pressure drop along the upstream and the singularity pipes are compared with the results computed by the correlations existing in the literature, in this section. In two-phase flow, pressure drop has three components, as written below.

$$\Delta P_{total} = \Delta P_{static} + \Delta P_{momentum} + \Delta P_{friction} \tag{11}$$

For the upstream pipe, it can be stated that the friction pressure drop ($\Delta P_{friction}$) is the dominant parameter since the pipe is horizontal and the mass flow rate of the flow through the pipe is constant. For the singularity pipe, in addition to the frictional pressure drop, momentum pressure drop is also important due to the deceleration caused by the enlarging singularity. The correlations used to evaluate the friction and the momentum pressure drops are listed in below equations.

$$\Delta P_{friction} = \Phi_L^2 \Delta P_L \tag{12}$$

$$\Delta P_L = 4 f_L \left(L / d_i\right) G_L^2 \left(1/2\rho_L\right) \tag{13}$$

$$f_L = 0.079 / \mathrm{Re}_L^{0.25} \ \textit{where}\ \mathrm{Re} = G_L d_i / \mu_L \tag{14}$$

$$\Phi_L^2 = 1 + C/X + 1/X^2 \ \textit{for}\ \mathrm{Re}_L > 4000 \tag{15}$$

$$X = \left(\frac{1-x}{x}\right)^{0.9} \left(\frac{\rho_G}{\rho_L}\right)^{0.5} \left(\frac{\mu_G}{\mu_L}\right)^{0.1} \tag{16}$$

$$\Delta P_{momentum} = G^2 \frac{d}{dz}\left(\frac{1}{\rho_m}\right) - \frac{G^2}{\rho_m} \frac{1}{A} \frac{dA}{dz} \tag{17}$$

Eq. 12 to Eq. 16 are proposed by Lockhart and Martinelli (1949). In Equ. 15, C depends on the flow regimes of the phases and takes the values given in Table 2.

Table 2. Values of C

Liquid	**Gas**	**C**
Turbulent	Turbulent	20
Laminar	Turbulent	12
Turbulent	Laminar	10
Laminar	Laminar	5

The pressure drop through the smooth enlargement is estimated with the correlation proposed by Kourakos et al (2009).

$$\Delta P_{\sin gularity} = \left[0.061 \cdot \alpha^{0.8917} - 10717 \cdot \mathrm{Re}_{L1}^{-0.8283} + 0.378\right] \times \frac{G_1^2}{2\rho_L}(1-\sigma)^2 \left[1 + x\left(\frac{\rho_L}{\rho_G} - 1\right)\right] \quad (18)$$

The numerical and calculated values of the pressure drop in the flow are given for $\beta = 21.74$ % and $\beta = 25.31$ % in Figure 18 and Figure 19, respectively.

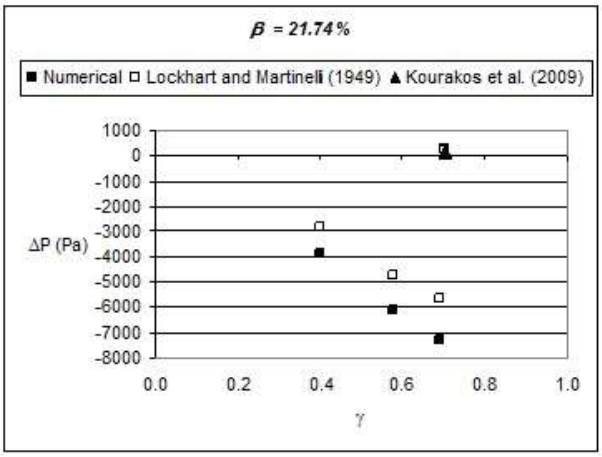

Figure 18. Pressure drop for $\beta = 21.74$ %

Once compared with the results computed by Lockhart and Martinelli (1949), it can be stated that the numerical model overestimates the pressure drop along the upstream pipe within a range between 21-25 %. The model utilized here is derived for fully developed, stratified flow, which does not take the entrance effects and developing flow conditions into consideration. However, in the numerical study, air-water flow is developing and stratifying along the upstream channel beyond outlet of the injector. Besides, in the numerical study, the surface roughness for the pipes is not taken into consideration considering that the pipes used in the experimental study are made of acrylic and "*roughness / diameter*" (ε / D) ratio is too small. Therefore, the error within a range in 21-25 % can be considered as acceptable for the case investigated. The numerical results for the pressure drop through the singularity are close to the estimations by Lockhart and Martinelli (1949) and Kourakos et al. (2009) within a range of 9-19 % and 14-37.5 %, respectively. It must be noted that the greater discrepancy stands for a flow with higher volumetric void fraction for all cases mentioned.

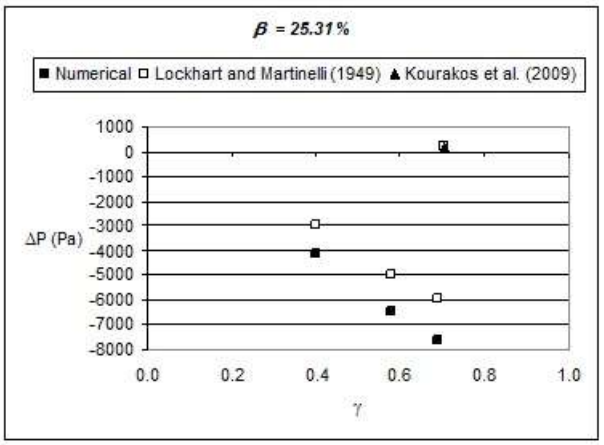

Figure 19. Pressure drop for $\beta = 25.31$ %

The effect of volumetric void fraction on two-phase pressure drop is illustrated with the numerical values plotted in Figure 20. As expected, the pressure drop increases by increasing volumetric void fraction.

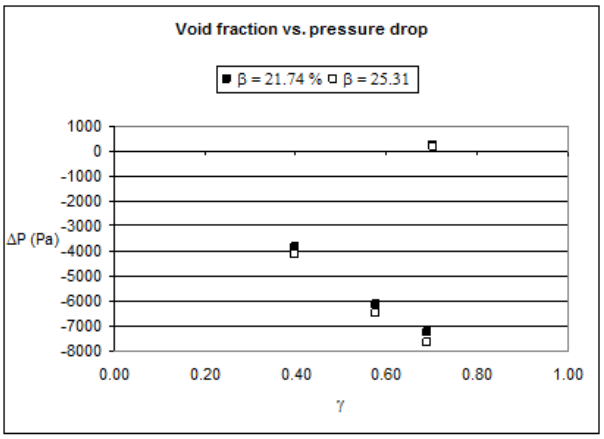

Figure 20. Pressure drop with respect to void fraction

CONCLUSIONS

In this study, the characteristics of air-water flow through the horizontal pipe with smooth expansion are investigated numerically and experimentally. According to the experimental results, it is concluded that the local void fraction increases with increasing y / D value due to the density difference between air and water, and the effect of gravitational force. The local void fraction increases with increasing volumetric void fraction and the effect of volumetric void fraction is more clearly observed at the top of the channel due to the development of stratification. It is found that the numerical and experimental values are comparable and

are getting closer to each other as the flow develops. The discrepancy mostly occurs at the bottom half of the channel since the numerical stratification develops earlier than the experimental stratification. Void fraction distribution through the singularity pipe takes the shape of a curve due to deceleration of the water is greater than deceleration of the air. The slip ratio between the phases varies between 1.24 and 0.58 in the flow though the pipes. Thus, the separated flow model must be employed in order to analyze the characteristics of the flow, as is performed in the present study. The numerical model overestimates the pressure drop in the flow compared to the results calculated by the correlations provided in literature (Lockhart and Martinelli 1949, Kourakos et al. 2009).

ACKNOWLEDGEMENT

We would like to express our appreciations to von Karman Institute for Fluid Dynamics, and Prof. J. M. Buchlin, Assoc. Prof. Patrick Rambaud, and Dr. Vasilis Kourakos for their support and cooperation during the experimental study.

REFERENCES

Ahmed W. H., Ching C. Y. and Shoukri M., 2008. Development of Two-Phase Flow Downstream of a Horizontal Sudden Expansion, *Int. J. Heat Fluid Flow*. 29, 194-206.

Aloui F., Doubliez L., Legrand J. and Souhar M., 1999, Bubbly Low in an Axisymmetric Sudden Expansion: Pressure Drop, Void Fraction, Wall Shear Stress, Bubble Velocities and Sizes, *Exp. Therm Fluid Sci*., 19, 118-130.

Balakhrisna T., Ghosh S., Das G. and Das P. K., 2010, Oil-Water Flows through Sudden Contraction and Expansion in a Horizontal Pipe – Phase Distribution and Pressure Drop, *Int. J. Multiphase Flow*, 36, 13-24.

Bertola V.,2004, The Structure of Gas-Liquid Flow in a Horizontal Pipe with Abrupt Area Contraction, *Exp. Therm Fluid Sci*., 28, 505-512.

Chahed J., Roig V., Masbernat L., 2003, Eulerian-Eulerian Two-Fluid Model for Turbulent Gas-Liquid Bubble Flows, *Int. J. Multiphase Flow*, 29, 23-49.

Deniz E.,2009, *Experimental Study of Bubbly Flow in Singular Geometries (Research Project Report 2009-09)*, VKI Library, Belgium.

Ekambara K., Sanders R. S., Nandakumar K. and Masliyah J. H., 2008, CFD Simulation of Bubbly Two-Phase Flow in Horizontal Pipes, *Chem. Eng. J.*, 144, 277-288.

Fossa M. and Guglielmini G., 1998, Dynamic Void Fraction Measurements in Horizontal Ducts with Sudden Area Contraction, *Int. J. Heat Mass Transfer*, 41, 3807-3815.

François F., Garnier J. and Cubizolles G., 2003, A New Data Acquisition System for Binary Random Signal Application in Multiphase Flow Measurements, *Meas. Sci and Tech.*, 14, 929-942.

Ghorai S. and Nigam K. D. P., 2006, CFD Modeling of Flow Profiles and Interfacial Phenomena in Two-Phase Flow in Pipes, *Chem. Eng. Process*, 45, 55-65.

Kourakos V. G., Rambaud P., Chabane S. and Buchlin J. M., 2009, Modeling of Pressure Drop in Two-Phase Flow within Expansion Geometries, *AIP Conf. Proc.*, 1207, 802-80.

Kunii D., 1991, *Fluidization Engineering*, Butterworth-Heinemann, Boston.

Lockhart R. W. and Martinelli R. C., 1949, *Chem. Eng. Prog*., 45, 39-48.

Morel C., Ruyer P., Seiler N. and Laviéville J. M., 2010, Comparison of Several Models for Multi-Size Bubbly Flows on an Adiabatic Experiment, *Int. J. Multiphase Flow*, 36, 25-39.

Winterton R. H. S. and Munaweera J. S., 2001, Bubble Size in Two-Phase Gas-Liquid Bubbly Flow in Ducts, *Chem. Eng. Process*, 40, 437-447.